VISUALIZATION OF COPPER IN TREATED WOOD USING X-RAY MICRO-COMPUTED TOMOGRAPHY

P.D. Evans[1,2], A.J. Limaye[3], M. Turner[2], T.J. Senden[2], M.A. Knackstedt[2]

[1]Centre for Advanced Wood Processing, University of British Columbia, Vancouver, V6T 1Z4, Canada
[2]Department of Applied Mathematics, The Australian National University, Canberra, ACT 0200, Australia
[3]Visualization Laboratory, The Australian National University, Canberra, ACT 0200, Australia

Summary

This study tests the hypothesis that X-ray micro-computed tomography (CT) will be able to visualize the spatial distribution of copper in wood treated with a micronized wood preservative. A small wood block wood measuring 12 x 12 x 19 mm was cut from a 2.4 m x 51 x 51 mm southern pine batten that had been commercially treated with a micronized wood preservative. Tomograms of the wood block were obtained using an X-ray micro-CT device over a period of 14 hours, and the phases in tomographic images with different densities were identified. These phases, which corresponded to wood (earlywood and latewood), void space and copper were visualized in 2 and 3 dimensions using volume rendering software. We observe that copper accumulates in rays and resin canal where it forms a grid-like network, particularly in the first two growth rings near the surface of the treated wood block. Less copper is present in subsequent growth rings because fewer rays and resin canals are filled with copper. We conclude that X-ray micro-CT is a useful technique for visualizing the spatial distribution of copper in wood treated with a micronized wood preservative. Future research will use X-ray micro-CT to visualize the distribution of copper in wood's finer capillary network, and we also plan to use various numerical techniques to quantify the distribution of copper in the microstructure of treated wood.

1. Introduction

The performance of wood preservatives depends, in part, on their ability to penetrate wood's complex microstructure and also the cell walls of tracheids and parenchyma (Arsenault 1973). Hence, soon after micronized wood preservatives were commercialised, research was undertaken to examine the microdistribution of copper carbonate particles in southern pine treated with a micronized wood preservative (Matsunaga et al. 2008, 2009). Scanning electron microscopy revealed that copper carbonate particles accumulated in rays, resin canals, pit borders and, to a lesser extent, tracheid lumens of treated wood (Matsunaga et al. 2008, 2009). High resolution transmission electron microscopy revealed that copper was present in the cell walls of tracheids and parenchyma cells as ions or atoms (Matsunaga et al. 2009, 2010). Transmission electron microscopy also revealed that small copper carbonate nanoparticles (< 2 nm in diameter) were able to penetrate the cell walls of non-lignified parenchyma cells, but were excluded from tracheid walls (Matsunaga et al. 2010). Electron microscopy is not very good at revealing the spatial distribution of metals in materials, and important questions remain about the distribution of micronized preservatives in wood. For example, are their differences in the distribution of copper carbonate in earlywood and latewood tissues and how does the spatial distribution of

copper carbonate vary centripetally within the wood? To answer these questions we turned to X-ray micro-computed tomography.

X-ray computed tomography is commonly used to diagnose diseases of soft and hard tissues, and detect defects in the turbine blades of jet engines or the rotor blades of helicopter (Hanke et al. 2008, Wang et al. 2008). X-ray micro-CT is a related technology, but it has higher resolution thanks to the availability of high-brilliance X-ray sources, high resolution X-ray detector systems, efficient algorithms for image processing and powerful software and hardware for 3-D visualization. X-ray micro-CT has been used to image a range of porous materials including bone, rock, coral and some man-made materials including foam and paper (Sakellariou et al. 2007). High resolution 3-dimensional images of wood and wood composites have also been published (Alemdar et al. 2008, Walther and Thoemen 2009, Wang et al. 2007). One of these studies used gold as a contrast agent (Wang et al. 2007). In our previous work we used copper to label a melamine-urea formaldehyde adhesive in particleboard and, as a result, we were able to visualize and quantify the distribution of the adhesive in particleboard (Evans et al. 2010). Accordingly, we hypothesize here that X-ray micro-CT will be able to visualize the distribution of copper in wood treated with a micronized wood preservative containing copper carbonate. In this paper we test this hypothesis by using use X-ray micro-CT to characterize the spatial distribution of copper in southern pine wood treated with a micronized wood preservative.

2. Materials and Methods

Five southern pine wood samples measuring 2.4 m x 51 x 51 mm and treated with micronized wood preservative were purchased commercially. Specimens measuring 25.4 x 51 x 51 mm were cut from the centre of each sample. One specimen with growth rings oriented parallel and perpendicular to its surfaces was selected and a small block of wood measuring 12 x 12 x 19 mm was cut from this specimen (Fig 1.). A separate wood block was cut from the same specimen and its copper content was measured using X-ray fluorescence spectroscopy (AWPA 2004).

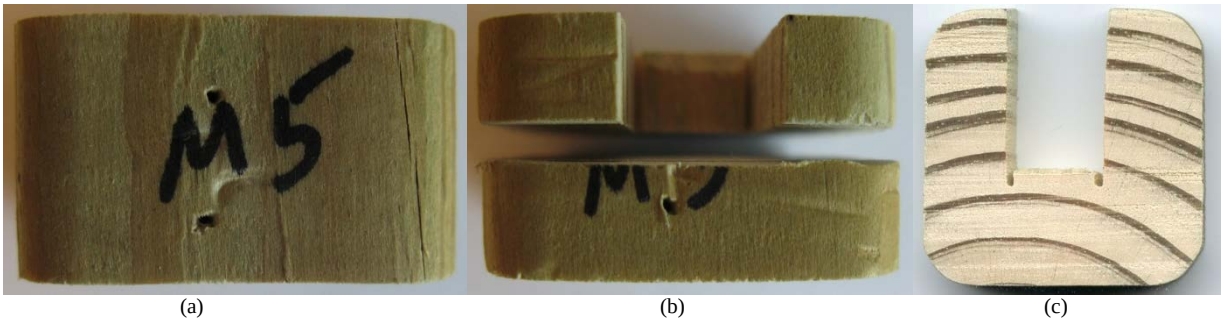

(a) (b) (c)

Figure 1. Southern pine sample treated with a micronized wood preservative: (a) Sample measuring 25.4 x 51 x 51 mm. Note the small holes created by a staple that was used to fix a label to the sample; (b) Specimen showing the saw cuts made to create a small block measuring 12 x 12 x 19 mm; (c) Cross-section through the specimen showing the number and orientation of growth rings in the specimen and the rectangular space created by the removal of the small block

The treated wood block was imaged using an X-ray micro-CT device built by the Department of Applied Mathematics within the Research School of Physics and Engineering at The Australian

National University. The X-ray micro-CT device is 3 m long and consists of an X-ray source (X-Tek RTF-UF225), rotation stage (Newport RV120PP) and X-ray camera (Roper PI-SCX100:2048) mounted on a parallel optical rail (Sakellariou et al. 2004). These features give the device a large field of view (20483 [8 billion] voxels [three-dimensional points in the tomogram] and 55 mm cross-section), good spatial resolution (down to 2 μm depending on operating voltage) and high dynamic range for enhanced contrast (16 bits) (Sakellariou et al. 2004). The treated wood block was placed on the rotation stage and probed with a polychromatic X-ray beam (breaking radiation or Bremsstrahlung, 30–225 kV/1 mA with 2–5 μm spot size) generated by a focused electron beam (40 kV and beam current of 200 mA) and blanked with a 2.5 mm platinum shutter. A CCD camera recorded the X-ray transmission radiograph, and a series of radiographs, collectively called the projection data, were collected by rotating the specimen stage through 360°. The optimum number of projections, N_θ is given by $N_\theta=(\pi/2)N_w$, where N_w is the number of pixels in the width of the detector. Projection data were processed with a Feldkamp reconstruction algorithm to generate a tomogram (Feldkamp et al. 1984), which is a three-dimensional representation of the variation in density within the specimen. It took approximately 14 h to acquire the tomographic images for the specimen. The quality of these tomograms was optimized using a range of measures to overcome the limitations imposed by using a polychromatic X-ray cone beam. These included pre-filtering the X-ray beam to minimize beam hardening, and using a small cone beam angle (0.8°). Pre-filtering typically uses a filter with a similar composition to the specimen and a thickness of about 37% (e^{-1}) of the diameter of the specimen. The projection data must represent linear interactions between the specimen and the X-rays to generate a tomogram. For X-ray tomography, however, the interaction is not linear because X-rays are attenuated, but Beer's law can accurately describe such attenuation and can be easily manipulated into a linear form, provided the X-ray beam is mono-energetic. This linearization also works with the poly-energetic X-rays employed in our instrument, but beam hardening artifacts are introduced into the tomogram. These artifacts were minimized by reducing the energy distribution of the X-rays using pre-filtering, as mentioned above. Artifacts can also be introduced into the tomogram by cosmic rays, defects, non-linear sensitivity and spatial non-linearity in the X-ray camera, misaligned cone beam geometry and specimen rotation and variability of the X-ray flux from the source. A full description of these problems and the algorithms implemented to reduce their effects is beyond the scope of this paper. Three-dimensional volumes were used to generate intensity histograms for void, wood and copper within the treated wood specimen. Thresholding of the peaks in these intensity histograms allowed the different phases in the tomographic image to be identified at a resolution of 8 ± 1 μm. Data sets were visualized in 2 and 3-D using volume rendering in which a transfer function assigns each voxel a colour and transparency (Knackstedt et al. 2006). Volume rendering was performed using the software Drishti, which is an open source volume exploration and presentation tool for visualizing tomographic data and is available at http://code.google.com/p/drishti-2/downloads/list.

3. Results and Discussion

The retention of copper in the matched wood block that was analyzed using X-ray fluorescence spectroscopy was 0.59 % (w/w). The distribution of copper in the treated wood blocks can be seen in 2-D images selected from full tomographic sequences (Fig. 2a–c). Figure 2a shows a

transverse section of the treated block. Colour is used to highlight different tissue types and show where copper is located in the section. Lower density earlywood tissue in growth rings is light grey (Fig. 2a). Higher density latewood is a darker grey and copper is fluorescent green (Fig. 2a). The different anatomical feature of the wood can be seen with reference to Figure 1. There is part of a band of earlywood at the top of the section. Below this partial earlywood band there is a complete growth ring consisting of the first band of latewood in the top of the image and an adjacent band of earlywood. Embedded in this band of earlywood is a thin band of latewood, possibly a false growth ring. Thereafter there are two complete growth rings each containing earlywood and latewood bands, and a partial growth ring at the bottom of the image. The pattern of growth is from the bottom of the image to the top. The same pattern of growth rings can be seen in Fig. 1c. Figure 2 consists of three images showing transverse, radial longitudinal and tangential longitudinal sections through the treated wood block. All three images show that copper is found at high concentrations in large fusiform rays running perpendicular to the growth rings and within vertical resin canals, mainly located in latewood. The accumulation of copper in resin canals explains in part the high concentration of copper at the interface between latewood and earlywood (Fig. 2b,c). Some resin canals are devoid of copper and this is particularly noticeable in the two lower bands of latewood in the transverse section in Figure 2a.

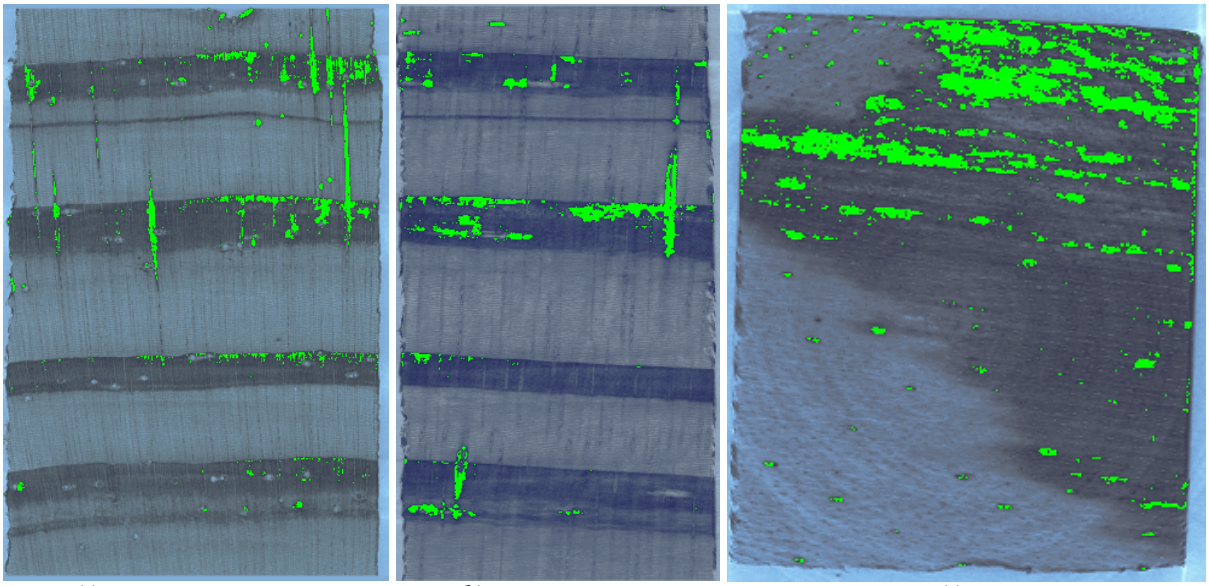

(a) (b) (c)

Figure 2. Images from a treated southern pine block showing the location of copper (green) within the wood's microstructure: (a) Transverse section showing copper located in fusiform rays running from top-to-bottom and within vertical resin canals in the darker bands of latewood; (b) Radial longitudinal section showing copper located in rays running from top to bottom and within resin canals in latewood (running from left to right). Note the accumulation of copper in the last formed latewood in the second full growth ring; (c) Tangential longitudinal section at the interface between the lighter coloured earlywood of the first growth ring and the darker colored last formed latewood of the second growth ring. Copper is concentrated in the rays that appear as small flecks and in resin canals in latewood running from left to right

The static images shown in Figure 2 are not very good at showing the spatial distribution of copper in the sample. Therefore 3-D animations showing the distribution of wood, void and

copper in the sample were produced. Figure 3a–c shows images from one of these animations. Figure 3a shows an image of the entire treated wood block. Four bands of light brown, higher density latewood, can be seen corresponding to the four dark bands within the original wood block shown above in Fig. 1c.

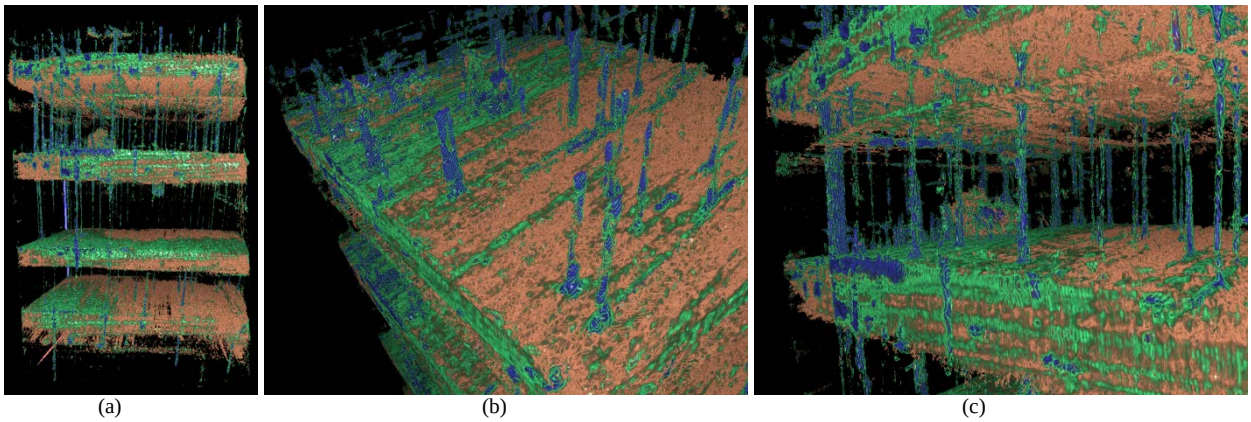

(a) (b) (c)

Figure 3. Images showing the location of high concentrations of copper in the earlywood of a treated wood block imaged using X-ray micro-computed tomography: (a) Image of the whole wood block (also see Fig. 1c, above) showing copper (blue and green) and four bands of brown latewood. The earlywood is transparent to allow copper to be seen in this tissue type; (b) Close-up view of the top of the treated wood block showing pillars of copper (blue/green) located within the first band of low density earlywood and also the accumulation of copper at the interface between latewood and earlywood (top left); (c) Close-up of pillars of copper in the second band of earlywood.

A thin band of latewood, possibly a false growth ring, can be seen below the first band of latewood in Fig. 3a. This thin band of latewood can also be seen in the second band of earlywood in the wood block shown above in Fig 1c. The bands of earlywood in Fig. 3 are transparent allowing higher density copper to be easily visualized. Higher density regions of copper are colored blue and lower density regions are colored green. Numerous pillars of copper run radially from the top of the specimen to the bottom (Fig. 3a,b). These pillars of copper are occasionally contiguous running across a number of bands of latewood (Fig. 3a) and appear to result from the accumulation of copper within the rays (compare Fig. 3a and Fig. 1c). Copper also accumulates at the interface between earlywood and latewood (Fig. 3b) and occasionally in tubes that run at right angles to the copper in the rays. One of these tubes of copper can be seen in the second band of earlywood in Fig. 3c (left of centre). The second band of earlywood in Fig. 3c also contains a small mound of wood. This mound of wood sits on the second band of latewood and is connected to the surface of the wood block by a diagonally angled hole created by the staple prong that was used to fix a label to the sample (Fig. 4a). Figure 4b shows an image of a single band of earlywood, and better shows the grid-like pattern of accumulation of copper in the rays (running radially from top to bottom), and in three resin canals that run perpendicular to the rays. Resin canals are more common in the latewood of *Pinus* sp (Blanche et al. 1992). Therefore latewood was also made optically transparent to better see the distribution of copper in this tissue type (Fig. 5).

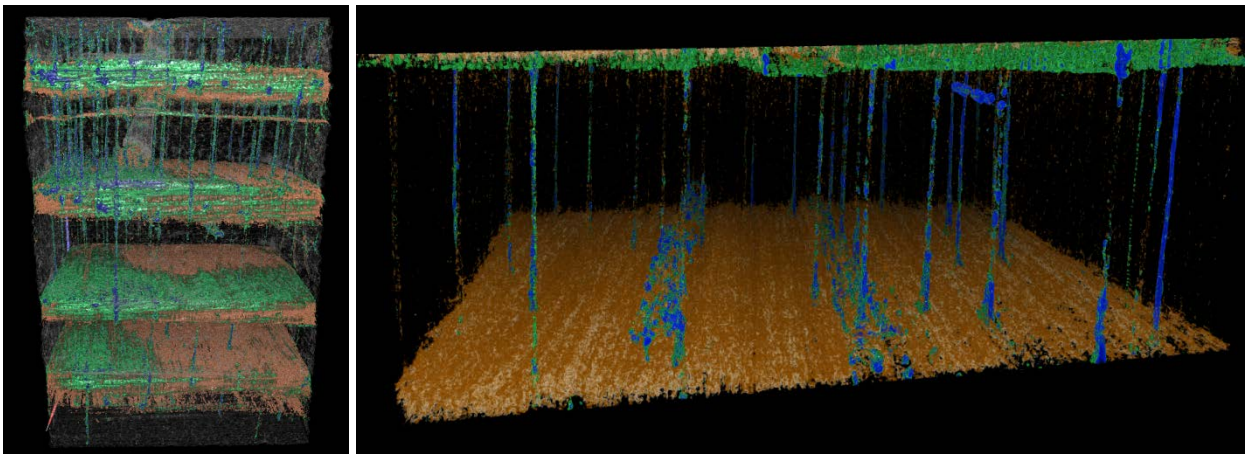

(a) (b)

Figure 4. (a) Image of the whole wood block (see Fig. 1c) showing copper (blue and green), four bands of brown latewood and a hole that penetrates the first band of latewood. A mound of wood lies at the bottom of this hole; (b) Image of a band of earlywood showing copper in rays running from top to bottom and copper in three resin canals running perpendicular to the rays

Figure 5a shows the entire block of treated wood that was imaged using X-ray micro-CT. Four bands of brown, lower density, earlywood, can be seen corresponding to the four lighter bands within the original wood block shown above in Fig. 1c. The latewood in the images is optically transparent allowing green colored copper to be seen within the latewood (Fig. 5). The first two bands of latewood contain a large amount of copper resulting from the accumulation of copper in rays and resin canals (Fig. 5a-b). Less copper is present in the subsequent bands of latewood because fewer rays and resin canals contain copper (Fig. 5c).

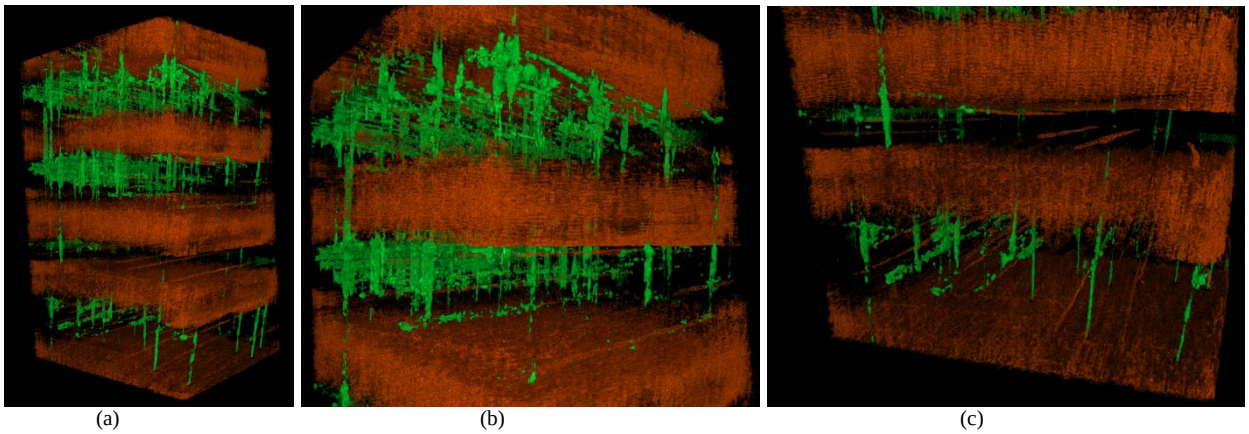

(a) (b) (c)

Figure 5. Images showing the location of high concentrations of copper in the latewood of a treated wood block imaged using X-ray micro-computed tomography: (a) Image of the whole wood block (compare with Fig. 1c, above) showing copper (green) and four bands of brown earlywood. The latewood is transparent to allow copper to be seen in this tissue type; (b) Close-up of the first two bands of latewood containing large amount of copper due to the accumulation of copper in the rays and resin canals; (c) Close-up of copper in the third and fourth bands of latewood. Note that less copper is present in these bands of latewood because fewer rays and resin canals contain copper

This study has shown that X-ray micro-CT is a useful technique for visualizing the spatial distribution of copper in wood treated with a micronized wood preservative. The technique has confirmed earlier observations that copper accumulates in rays and resin canals where it forms a grid-like network particularly in growth rings near the surface of treated wood. Within these growth rings more copper appeared to be present in latewood than in earlywood because latewood contained more resin canals filled with copper compared to earlywood. Copper was not detected in bordered pits, because our sample was scanned at a resolution of 8 ± 1 μm, which is insufficient to visualize wood's finer capillary network. However, we intend to analyze the wood block at a higher resolution to detect copper in bordered pits, and also use a variety of numerical techniques to quantify the spatial distribution of copper in the wood's micro-structure.

4. Conclusions

X-ray micro-computed tomography was able to visualize copper in the rays and resin canals of southern pine wood that had been treated with a micronized wood preservative. These observations confirm previous findings made using scanning electron microscopy. X-ray micro-computed tomography also revealed that copper in rays and resin canals forms a grid-like network particularly in the first two growth rings near the surface of treated wood. Within these growth rings more copper appeared to be present in latewood than in earlywood because latewood contained more resin canals filled with copper compared to earlywood. Fewer rays and resin canals were filled with copper in growth rings that were further from the outer treated surfaces. We conclude that X-ray micro-CT is a useful technique for visualizing the spatial distribution of copper in wood treated with a micronized wood preservative. Future research will use X-ray micro-CT to visualize the distribution of copper in wood's finer capillary network, and also use numerical techniques to quantify the spatial distribution of copper in treated wood.

5. Literature

Alemdar, A., Zhang, H., Sain, M., Cescutti, G., Mussig, J. 2009. Determination of fiber size distributions of injection moulded polypropylene/natural fibers using X-ray microtomography. Advanced Engineering Materials. 10(1-2):126-30.

Arsenault, R.D. 1973. Factors influencing the effectiveness of preservative systems. In: Wood Deterioration and Its Prevention by Preservative Treatments, D D Nicholas (ed.). Vol 2, pp 121-278. Syracuse University Press, New York.

AWPA 2004. Standard method for analysis of treated wood and treating solutions by X-ray spectroscopy. Standard A9-01. AWPA Book of Standards, Birmingham, AL.

Blanche, C.A., Lorio Jr., P.L., Sommers, R.A., Hodges, J.D., Nebeker, T.E. 1992. Seasonal cambial growth and development of loblolly pine: xylem formation, inner bark chemistry, resin ducts, and resin flow. Forest Ecology and Management. 49(1-2):151-165.

Evans, P.D., Matsunaga, H., Kiguchi, M. 2008. Large-scale application of nanotechnology for wood protection. Nature Nanotechnology. 3(10):577.

Evans, P.D., Morrison, O., Senden, T.J., Vollmer, S., Roberts, R.J., Limaye, A., Arns, C.H.,

Averdunk, H., Lowe, A., Knackstedt, M.A. 2010. Visualization & numerical analysis of adhesive distribution in particleboard using X-ray micro-computed tomography. International Journal of Adhesion & Adhesives. 30(8):754-762.

Feldkamp, L.A., Davis, L.C., Kress, J.W. 1984. Practical cone-beam algorithm. Journal of the Optical Society of America A: Optics, Image Science, and Vision. 1(6):612-619.

Hanke, R., Fuchs, T., Uhlmann, N. 2008. X-ray based methods for non-destructive testing and material characterization. Nuclear Instruments and Methods in Physics Research Section A: Accelerators, Spectrometers, Detectors and Associated Equipment. 591(1):14-18.

Knackstedt, M.A., Arns, C.H., Saadatfar, M., Senden, T.J., Limaye, A., Sakellariou, A., Sheppard, A.P., Sok, R.M., Schrof, W., Steininger, H. 2006. Elastic and transport properties of cellular solids derived from three-dimensional tomographic images. Proceedings of the Royal Society A-Mathematical Physical and Engineering Sciences**.** 462(2073):2833-2862.

Matsunaga, H., Kiguchi, M., Roth, B., Evans P.D. 2008. Visualisation of metals in pine treated with preservative containing copper and iron nanoparticles. International Association of Wood Anatomists Journal. 29(4):387-396.

Matsunaga, H., Kiguchi, M., Evans P.D. 2009. Microdistribution of copper-carbonate and iron oxide nanoparticles in treated wood. Journal Nanoparticle Research. 11(5):1087-1098.

Matsunaga, H., Kataoka, Y., Kiguchi, M., Evans, P.D. 2010. Copper nanoparticles in southern pine wood treated with a micronised preservative: Can nanoparticles penetrate the cell walls of tracheids and ray parenchyma? International Research Group on Wood Protection Document IRG/WP 10-30547.

Sakellariou, A., Arns, C.H., Sheppard, A., Sok, R.M., Averdunk, H., Limaye, A.J., Jones, A.C., Senden, T.J., Knackstedt, M.A. 2007. Developing a virtual materials laboratory. Materialstoday. 10(12):44-51.

Sakellariou, A., Sawkins T., Senden, T.J., Limaye, A. 2004. X-ray tomography for mesoscale physics applications. Physica A: Statistical Mechanics and its Applications. 339(1-2):145-51.

Walther, T., Thoemen, H. 2009. Synchrotron X-ray microtomography and 3D image analysis of medium density fiberboard (MDF). Holzforschung. 63(5):581-587.

Wang, G., Yu, H., De Man, B. 2008. An outlook on x-ray CT research and development. Medical Physics. 35(3):1051-1064.

Wang, Y., Muszynski, L., Simonsen, J. 2007. Gold as an X-ray CT scanning contrast agent: effect on the mechanical properties of wood plastic composites. Holzforschung. 61(6):723-730.